

# A Probabilistic Model for the Dynamics of Cascading Failures and Blackouts in Power Grids

Mahshid Rahnamay-Naeini\*, Zhuoyao Wang\*, Andrea Mammoli†, and Majeed M. Hayat\*‡

E-Mail: mrahnama@ece.unm.edu, zywang@unm.edu, mammoli@unm.edu, hayat@ece.unm.edu

\*Department of Electrical and Computer Engineering, University of New Mexico, Albuquerque, NM, USA

† Department of Mechanical Engineering, University of New Mexico, Albuquerque, NM, USA

‡ Center for High Technology Materials, University of New Mexico, Albuquerque, NM, USA

**Abstract**—Current power grids suffer periodic disturbances that may trigger cascades of component failures, which, in turn, can result in blackouts of different scales. Understanding cascading failures and the ability to predict the risk of blackouts are therefore of great value in designing control and outage management systems for future smart grids. In this paper, a novel probabilistic approach is proposed to model the dynamics of cascading failures in power grids. The model characterizes the probability of reaching a blackout of an arbitrary size in any time interval starting from an initial grid state. The model exploits two power grid parameters: the maximum capacity of the set of failed lines and the grid loading ratio. Simulations have shown that these parameters largely affect the cascading failures. In addition, the number of failed lines and the maximum capacity of the failed lines are utilized to reduce the space of all possible grid configurations into a much smaller set of equivalence classes, thereby making the model scalable to large power grids. The results of the analytical model are in agreement with Monte Carlo simulations performed with the IEEE 118-bus system.

**Index Terms**—power grid, smart grid, cascading failures, blackout, regeneration, blackout probability

## I. INTRODUCTION

Reliability is among the most desirable attributes of future smart grids. Quantitative and predictive knowledge of the effects of various disturbances on power grids are required to design future smart grids with robust control and outage management systems. The control system of a reliable power grid requires (1) a good understanding of the current state of the grid and (2) good prediction and estimation capabilities of the risk of blackout in order to take necessary corrective actions to respond to a disturbance. The current infrastructure of power grids suffers periodic disturbances that may trigger a sequence of *dependent* component failures, which is termed cascading failure. Cascading failure is the usual mechanism for large blackouts of electric power transmission systems [1].

To this end, researchers have exerted considerable efforts in deriving models for cascading failures in power grids, with the ultimate goal of designing cascading-failure-aware control and outage management systems. However, detailed models of cascading failure blackouts are generally intractable since power grids are among the largest and most complex artificial systems ever developed [2]. Moreover, blackouts are particularly complex phenomena as they are attributable to a large number of interacting factors [3]–[5]. Specifically, both external (snow storms, hurricanes, lightning strikes, and attacks) and internal

(voltage instability, inadequate reactive power sources, human errors and failures in the control/communication systems) factors can affect cascading failures in power grids. These factors can cause failures of power system components such as transmission lines and generators, which, in turn, may lead to the isolation of parts of the transmission system. Each power component failure results in a power flow redistribution. New failures may occur at certain components as they become overloaded due to power flow redistribution [1], [6].

The complex nature of the problem has inspired many researchers to rely only on simplified abstract models to facilitate the understanding of cascading failures in power grids. While probabilistic approaches are well accepted in the literature [1], [2], [7]–[9], they often lack a strong connection to the physical characteristics of power grids. A challenge common to the abstract models is whether they can capture the key physical parameters of the grid while they keep the complexity to a minimum. On the other hand, scalability is the main challenge in the more realistic detailed models for cascading failures. This paper is an attempt to address both of these challenges by introducing a detailed probabilistic model for the dynamics of cascading failures in power grids, which exploits some of the key physical characteristics of power grids. This model is based on the concept of stochastic regeneration (generalization of renewals) [10], [11] and it characterizes the probability of reaching an arbitrary size blackout in any time interval following an initial “state” of the power grid.

We consider transmission line outages in our model since they are one of the simplest and most observable signs of cascading failures. However, the model can be extended easily to include any power grid component failure. Similar to the works in [7], [12], [13], we use the number of line outages to represent blackout size. Moreover, we have learned through detailed power grid simulations that in addition to ratio of the total load over the maximum generation capacity of the power grid [6], there are certain physical parameters whose role is particularly critical in cascading failures. These include the power transmission capacity of the failed lines and the maximum capacity of the set of failed lines, which effect, to a large degree, the dynamics of power flow redistribution and cascading failure blackouts in power grids.

With the number of failed lines and the maximum capacity of the failed lines identified as key characterizable factors governing cascading failures, they can collectively be used as

a criterion to partition the configuration space of power grids according to disjoint equivalence classes. This is a meaningful and powerful way to simplify (partition) the complex actual configuration space. We emphasize that the simplified configuration space, or state space, maintains only the key attributes of the configurations that are most relevant to cascading failures. Hence, scalable analytical modeling becomes possible for realistic large-scale power grids.

The remainder of this paper is organized as follows. In Section II we present a brief survey of the existing works in modeling cascading failures in power grids. In Section III we introduce the key features of power grids used in the model. The main theoretical concepts of the model are described in Section IV-A and the regeneration-based model for cascading failures is presented in Section IV-B. In Section IV-C, we estimate the model parameters using power system simulations. In Section V blackout probabilities are calculated using the regeneration-based model in conjunction with the estimated model parameters. Finally, our conclusions are presented in Section VI.

## II. PRIOR WORK

There has been a great volume of work in understanding and modeling cascading failure blackouts using deterministic and probabilistic dynamical models. Among the probabilistic models, the loading-dependent CASCADE model [1] and the branching-process-based model developed in [7]–[9] have gained more attention due to simplicity and consistency with the statistics of blackouts that have occurred in the last decades. The CASCADE model [1] is an analytically tractable probabilistic model, in which the authors assume a system of identical components with random initial loads. They assume that when a component fails, its load will be redistributed equally to all the other components in the system. A component failure occurs when its load exceeds a threshold. This mechanism captures a loading-dependent cascading failure in a system. However, this model does not consider the topological or electrical characteristics of power grids such as power flow redistribution following an outage and heterogeneous component capacity values.

The branching-process-based model presented in [7]–[9] provides an analytic formulation of the probability distribution of the total number of component failures. In this model, the failures occur randomly in a series of stages. The parameter set of the model includes the average number of initial failures and an average tendency for the failures to propagate. This model has the limitation that it does not have sufficient degrees of freedom to capture the physical factors contributing in cascading failures of the power grids. The tendency for the failures to propagate is the only (fixed) parameter used in the model and it can be estimated and tuned to the power grid data. As such, this parameter may not be sufficient to represent dynamic attributes of cascading failures since it does not consider changes in the state of the grid.

Examples of the deterministic approaches are [14], [15]. The work presented in [14] offers a model for cascading failures in complex networks. This work is motivated in part

by the propagation of failures and congestion in computer networks. The presented model for communication networks differs from power grid models in that it considers flows of fully controlled discrete packets of information, rather than flow of electricity in the power grid. Another example of the deterministic model is a hybrid nonlinear system model using Lyapunov methods that is proposed by DeMarco in [15] to determine cascading failures due to dynamic transients in the system. In this work a detailed RLC circuit model is used as an example to illustrate the concept of cascading failures in the context of RLC circuits. The deterministic approaches cannot capture the effects of stochastic events that affect cascading failures and they are not usually scalable to large systems. More comprehensive reviews on the models for cascading failures are available in the literature, see for example [16].

## III. NOTION OF POWER GRID STATE-SPACE BASED ON PARAMETERS THAT AFFECT CASCADING FAILURES

We refer to the health condition of the power grid, namely the status of every transmission line in the grid (operational or non-operational), as the *grid configuration*. We use the notation  $\mathcal{G}$  for the space of all the grid configurations. Now consider a power grid consisting of  $N$  buses (generators or substations) connected via  $L$  transmission lines. Note that line failures cause the power flow to be redistributed in the other lines of the power grid. The complexity of keeping track of grid configurations in conjunction with the power flow dynamics for modeling cascading failures is  $0.5L \times 2^L$ . This is because for each of the  $\binom{L}{m}$  configurations with  $m$  working lines, we associate  $m$  loads that flow through them. Hence, the complexity is calculated as  $\sum_{m=1}^L m \binom{L}{m} = 0.5L \times 2^L$ . This number is prohibitively large for power grids with thousands of transmission lines and can be even larger if the model needs to keep track of other parameters to achieve more accuracy. In this section, we motivate the use of certain power grid parameters identified through simulations, which play a critical role in the dynamics of load redistribution and cascading failures and help in reducing the complexity.

We use MATPOWER [17], a package of Matlab M-files, for conducting our power system simulations and solving optimal power flow problems throughout this paper. In our simulations, overloaded lines fail with probabilities corresponding to the amount of their overload. Note that the failed lines may result in the disconnection of some load and generation substations. Hence, the loads and the total power generated in the system may become imbalanced. In such scenarios load shedding is performed to balance the loads and generating power in the grid.

Based on our simulation results, both the *maximum capacity* of the failed lines and the *grid-loading ratio*,  $R_{D/G}$ , (which is defined as the ratio of the total demand over the total generation capacity of the grid) affect, to a large degree, cascading failures in power grids. Other system parameters, such as the shortage of reactive power sources, are known to be major factors in the evolution of cascading failures. However, transmission and generation capacity are the leading causes in

the early steps of cascading failures. We begin by showing the MATPOWER simulator results that clarify the importance of the role of the maximum capacity of the failed lines and the grid-loading ratio in cascading failures.

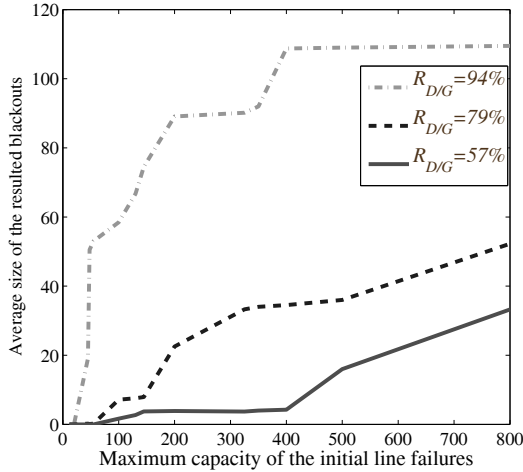


Fig. 1. Average size of blackouts, resulting from three initial line failures, as a function of maximum capacity of the initial line failures for three different grid-loading ratio.

Our simulation results over the IEEE 118-bus system are presented in Fig. 1. We assume that the set of capacity values of the transmission lines includes 18 different line capacity values based on length of the lines and their base voltage (we assume the range of 12 MW to the maximum line capacity of 850 MW [18]). We have simulated 10,000 random disturbances with three initial transmission line failures over the IEEE 118-bus system. The results suggest that maximum capacity of the failed lines is important in the severity of cascading failures. It is clear from the figure that the average size of the resulted blackouts increases with the maximum capacity of failed lines. Therefore, we propose using the maximum capacity of the failed lines in the model as an aggregated quantity in place of the entire collection of the capacity values of the failed lines in order to reduce complexity. Figure 1 also shows the effect of the grid-loading ratio on the average blackout size: when the system works close to its maximum generation capacity, the effect of any disturbance is intensified.

Now we explain the notion of power grid state space to be used in our model. We consider a finite set of line capacity values,  $\mathcal{C} = \{C_1, C_2, \dots, C_k\}$ , based on the transmission line attributes [18]. The use of number of failed lines and the maximum capacity of the failed lines as a descriptor of the “state” of the grid will enable us to partition the collection of all power grid configurations into a collection,  $\mathcal{S}$ , of equivalence classes. We will label each class,  $S \in \mathcal{S}$ , of grid configurations as a *grid state*, denoted by  $(C_{\max}, F)$ , where  $C_{\max}$  and  $F$  are the maximum capacity of the failed lines and the number of the failed lines in the grid, respectively. Note that the notion of partitioning the configuration space coarsely into “grid states” (or classes of configurations) implies that if two configurations have the same number of failed lines and the same maximum capacity of the failed lines then they belong to the same grid state. Hence they will be indistinguishable, in a coarse sense,

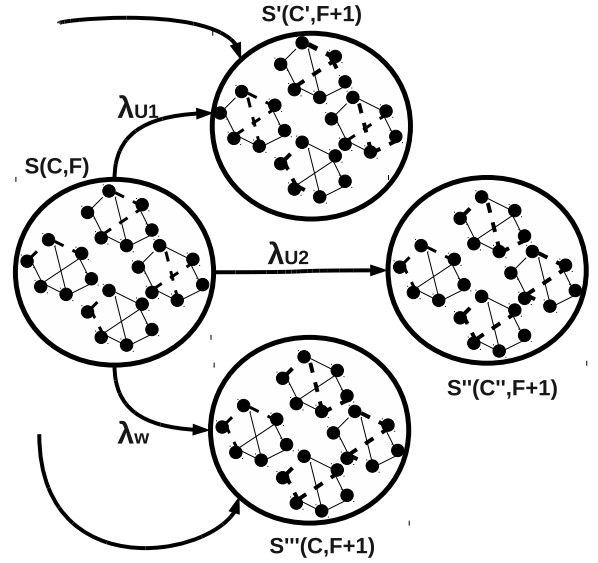


Fig. 2. Grid configuration, grid state and the transition between the grid states.

as far as cascading failures are concerned. This partitioning of the entire collection of grid configurations therefore reduces the complexity of tracking the dynamics of the power grid to  $kL$ . This is because instead of power flow dynamics in the lines for each configuration, we only consider the maximum capacity of the failed lines with  $k$  (the cardinality of set  $\mathcal{C}$ ) possible values and the number of the failed lines with  $L$  different values for each state. Therefore, this approach reduces the complexity from exponential to linear order in terms of the number of lines in the grid.

The concept of grid states and grid configurations is sketched in Fig. 2. Each large circle represents a grid state and the topological graphs with working and failed lines inside the circles representing different grid configurations with the same number of failures and the same maximum capacity of the failed lines. The notion of the grid states will be used in the analytical model for the probabilities of cascading failure blackouts which is discussed next.

#### IV. A PROBABILISTIC MODEL FOR DYNAMICS OF CASCADING FAILURES

Cascading failures in power grids may start with few initial failures. Natural disasters (earthquakes, snow storms, fires, etc.) as well as malicious attacks on the power grid are examples of events that can cause multiple simultaneous transmission line failures. To model cascading failures, we assume that the initial grid state contains at least one transmission line failure, otherwise there will be no cascading failure. In this model, we also assume that the initial state of the grid (the initial value of the pair  $(C_{\max}, F)$ ) is known. For instance, consider the case where the control system of the power grid (which is using the probabilistic model for estimating the risks of blackouts) obtains the number of initial failures and the maximum capacity of the initial failed lines as well as the grid-loading ratio through monitoring agents.

## A. PRELIMINARIES

When a single line failure occurs *after* an initial grid state  $S = (C_{\max}, F)$ , the grid state changes in one of the following ways. First, if the capacity of the newly failed line,  $C_f$ , is larger than  $C_{\max}$ , then the new grid state becomes  $S' = (C'_{\max}, F + 1)$  where  $C'_{\max} = C_f$ . Second, if  $C_f$  is smaller than or equal to  $C_{\max}$ , then the new grid state becomes  $S' = (C'_{\max}, F + 1)$  where  $C'_{\max} = C_{\max}$ . Hence, we can categorize the events that transpire after a line failure, starting from state  $S = (C_{\max}, F)$ , into two types. Note that any transition between the grid states is a probabilistic event because of the possible stochastic factors affecting cascading failures and also the fact that we do not know the exact grid configuration in the grid state. These events cause a single line outage thus the number of line failures,  $F$ , in the new grid state is incremented by one. We next characterize the transition probabilities and rates. Let  $U_i$  and  $W$  represent the time of the transition of state  $S = (C_{\max}, F)$  to state  $S' = (C_f, F + 1)$  for the case  $C_f > C_{\max}$  and to state  $S' = (C_{\max}, F + 1)$  for the case  $C_f \leq C_{\max}$ , respectively. The subscripts of the first random variable is for  $i \in \mathcal{I}$ , where  $\mathcal{I} \triangleq \{i | C_f = C_i, C_i \in \mathcal{C} \text{ and } C_i > C_{\max}\}$ . We assume throughout this paper that the random variables  $U_i$  and  $W$  are mutually independent and follow an exponential distribution with parameters (inverse of the mean)  $\lambda_{U_i}(S, R_{D/G})$  and  $\lambda_W(S, R_{D/G})$ , respectively. These parameters depend on the grid state and the grid-loading ratio,  $R_{D/G}$ . In this paper, we make the simplifying assumption that the load at a load bus is constant over the time interval that the cascading failures occur since the length of this interval is short. We assume that cascading failures develop over few hours and the interval between successive individual failures is shorter than that.

Depending on the actual configuration of the system, a grid configuration may behave differently (in a detailed sense) in the cascading failure. We call a power grid configuration *cascade-stable* if no line failures occur starting from that configuration. Since each class in the collection  $\mathcal{S}$  potentially contains multiple actual configurations, some of these possible configurations may be *cascade-stable*. Therefore, we define the *cascade-stability probability* for each state  $S \in \mathcal{S}$  as  $P_{\text{stab}}(S, R_{D/G})$ , which depends on the state of the system,  $S$ , and the grid-loading ratio,  $R_{D/G}$ . In words, *cascade-stability probability* specifies the probability that once the grid is in state  $S$  and grid-loading ratio is  $R_{D/G}$ , then it will remain stable in the same state  $S$ . To keep the model simple, we do not consider the effects of control actions in the cascading failures. The corrective and remedial control actions may affect the load over the grid, the cascade-stability probability, and transitions from the current grid state to the other states. However, the effects of certain control actions such as load shedding can be studied easily by changing the grid-loading ratio parameter in the model. Considering the effects of control actions can be an extension of this work.

## B. REGENERATIVE EQUATIONS

The idea of regeneration is that the occurrence of an event (in our case the first line failure in a grid state) regenerates,

or stochastically replicates, the same problem albeit with new initial conditions. The problem with the new initial condition is a completely independent problem and does not have any memory of the previous states other than the information embedded in the new grid state. The key point is to define a certain special random variable, called the *regeneration time*,  $\tau$ , defined as  $\tau \triangleq \min_i \{U_i, W\}$ , which represents the time to the first failure, or equivalently, the time of transition to a new state. From basic probability,  $\tau$  is also an exponential random variable with rate  $\lambda(S) = \sum_{i \in \mathcal{I}} \lambda_{U_i}(S) + \lambda_W(S)$ . To reiterate, the key feature of the event at time  $\tau$  is that its occurrence will regenerate the problem at  $\tau$ , which has the same statistical properties and dynamics as the original problem but with different initial configurations, viz., different number of failures with possibly different maximum capacity of the failed lines.

We use the notation  $B_{(C_{\max}, F)}^{R_{D/G}}(t, M)$  to represent the probability of reaching blackout size  $M$  or larger (a blackout with  $M$  or more line failures) in a time interval  $t$  and initial grid state  $S = (C_{\max}, F)$  and initial grid-loading ratio,  $R_{D/G}$ . Note that when  $F \geq M$  then  $B_{(C_{\max}, F)}^{R_{D/G}}(t, M) = 1$ . This is because the state has at least  $M$  failures and the probability of reaching a blackout state of size  $M$  or larger is one. Now, we consider the case  $F < M$  and derive integral equations describing the probability. By exploiting the properties of conditional expectations we can write,

$$B_{(C_{\max}, F)}^{R_{D/G}}(t, M) = (1 - P_{\text{stab}}(S, R_{D/G})) \times \int_0^t B_{(C_{\max}, F)}^{R_{D/G}}(t, M | \tau = s) f_{\tau}(s) ds, \quad (1)$$

where  $f_{\tau}(s)$  is the probability density function (pdf) of  $\tau$ .

Note that  $B_{(C_{\max}, F)}^{R_{D/G}}(t, M | \tau = s)$  is the probability of reaching a blackout with at least  $M$  failures in the time interval  $t$  conditioning on  $\tau$  being equal to  $s$  (first event occurs at  $s$ ). We write this probability as

$$\begin{aligned} & B_{(C_{\max}, F)}^{R_{D/G}}(t, M | \tau = s) = \\ & \mathbb{P}\{\tau = W | \tau = s\} B_{(C_{\max}, F)}^{R_{D/G}}(t, M | \tau = s, \tau = W) \\ & + \sum_{i \in \mathcal{I}} \mathbb{P}\{\tau = U_i | \tau = s\} B_{(C_{\max}, F)}^{R_{D/G}}(t, M | \tau = s, \tau = U_i). \end{aligned} \quad (2)$$

The conditional probabilities in (2) for the event  $\{\tau = U_i\}$  can be written as follows:

$$B_{(C_{\max}, F)}^{R_{D/G}}(T, M | \tau = s, \tau = U_i) = B_{(C'_{\max}, F+1)}^{R_{D/G}}(t - s, M). \quad (3)$$

Note that the conditional probability for the event  $\{\tau = W\}$  is similar to the one for event  $\{\tau = U_i\}$  except that  $C_{\max}$  of the new state is the same as the initial grid state. By following the steps presented in the appendix we can state theorem 1.

**Theorem 1** The probability of reaching a blackout of size  $M$  or larger in a time interval  $t$  and from an initial state  $S = (C_{\max}, F)$ , where  $F < M$ , and initial grid-loading ratio,  $R_{D/G}$ , is characterized by the following differential equation:

$$\begin{aligned}
\frac{dB_{(C_{\max}, F)}^{R_{D/G}}(t, M)}{dt} &= -\lambda(S, R_{D/G})B_{(C_{\max}, F)}^{R_{D/G}}(t, M) \\
&+ \left(1 - P_{\text{stab}}(S, R_{D/G})\right) \left(\lambda_W(S, R_{D/G})B_{(C_{\max}, F+1)}^{R_{D/G}}(t, M)\right) \\
&+ \sum_{i \in \mathcal{I}} \lambda_{U_i}(S, R_{D/G})B_{(C_{\max}, F+1)}^{R_{D/G}}(t, M).
\end{aligned} \tag{4}$$

Because the probability of reaching blackout for a grid state  $S$  is expressed based on the probability of reaching a blackout starting from another grid state  $S'$ , we have a set of coupled differential equations which must be solved simultaneously. The set of initial conditions for the differential equations is presented in (5). Note that when  $F \geq M$ , the probability of having a blackout of size  $M$  or larger is trivially equal to unity; therefore, the following initial conditions are imposed:

$$B_{(C_{\min}, C_{\max}, F)}^{R_{D/G}}(t, M) = 1, \text{ if } F \geq M. \tag{5}$$

Next we estimate model parameters to characterize the probability of blackouts for grid states.

### C. ESTIMATING MODEL PARAMETERS

The parameters to be estimated are the cascade-stability probabilities of the states,  $P_{\text{stab}}(S, R_{D/G})$ , and the transition rates,  $\lambda$ , between pairs of states. Our Monte Carlo simulations are performed using MATPOWER over the IEEE 118-bus and the IEEE 300-bus systems. We have simulated more than 20,000 cascading failures scenarios over each of the two test systems. In each of the scenarios we have few (less than 5) random line outages as the initial triggering event of the cascading failure. In our simulations, we keep track of the number of failures and the maximum capacity of the failed lines in each step of the cascading failure event and save the step as a state,  $S = (C_{\max}, F)$ , in our data set. We also save a binary variable termed *end-of-cascade* to mark the states in which cascade of failures stopped. The generated data set of the states enables us to estimate empirical probabilities of events and finally estimate the parameters of the model based on the simulations.

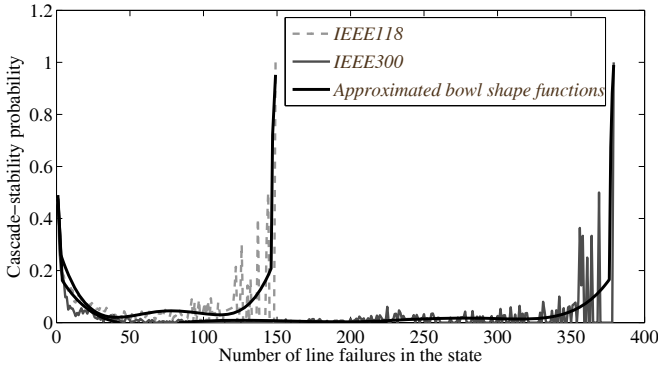


Fig. 3. Cascade-stability probability as a function of number of failures in the state.

First, consider the cascade-stability probability parameter in the model. Based on the simulation results presented in

Fig. 3, the grid states with very low or very large number of failures have higher probability of being cascade-stable. The IEEE 118-bus system has a total of 186 transmission lines and the IEEE 300-bus system has 411 transmission lines. Note that the cascade-stability probability has the same behavior in both grids as a function of number of failures. This observation can be explained by two points: (1) small-size blackouts are more probable than the large-size ones, and (2) not all the scenarios with small number of failures may trigger cascading failures and result in large blackouts. The probability of having the whole grid failure is also small. This can be because of the small functional power islands which are formed due to the line failures. Therefore, when a large fraction of the power grid fails, we can conclude that a “large” blackout has already occurred and the end of the cascading failure is imminent. Hence, we specify the cascade-stability probabilities of states as a function of their number of failures,  $Q_{P_{\text{stab}}}(F)$ , using a bowl-shaped function that approximates the data in Fig. 3.

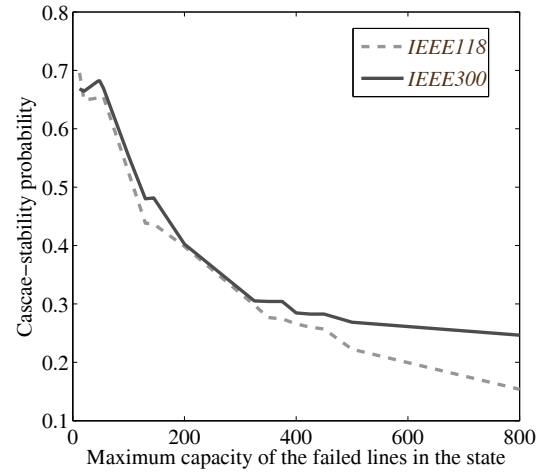


Fig. 4. Cascade-stability probability as a function of maximum capacity of the failed lines.

The results shown in Fig. 4 reveal the effect of maximum capacity of the failed lines on the cascade-stability probabilities of the grid states. As the maximum capacity of the failed lines increases, so does the probability that cascading failures continue. The function  $Y_{P_{\text{stab}}}(C_{\max})$  represents the cascade-stability probability as a function of maximum capacity of the failed lines in the grid states. This function can be fitted to the graph in Fig. 4. We have presented the effect of the grid-loading ratio on the size of the cascading failure blackouts in Section III. To consolidate the information on the number of line failures, the maximum capacity of the failed lines, and the grid-loading ratio we formed the probability,  $P_{\text{stab}}(S, R_{D/G})$ , which is vertically shifted versions of  $Q_{P_{\text{stab}}}(F)$  for different possible line capacity values. The amount of vertical shift is determined by function  $Y_{P_{\text{stab}}}(C_{\max})$  and  $R_{D/G}$ . Once the cascade-stability probability is determined, the probability that cascading failure continues is simply  $P_{\text{cas}}(S, R_{D/G}) = 1 - P_{\text{stab}}(S, R_{D/G})$ .

Next, we estimate the transition rates between pairs of states. To do so, we use our simulated data sets to first estimate the transition probability to various states and then calculate

the transition rates from the estimated transition probabilities. Conditioning on that the cascading failure continues from state  $S$ , we need to estimate the transition probabilities from state  $S$  to different possible states  $S'$ . Recall that in our model, line outages have been categorized into two types of transition events depending on the change in the  $C_{\max}$  of the new state. The two types of events are *change in  $C_{\max}$  event*,  $E_U$ , and *no change in  $C_{\max}$  event*,  $E_W$ . We first derive estimates of the probability of the event  $E_W$ ,  $P_{E_W}$ , and the probability of the event  $E_U$ ,  $P_{E_U}$ . Note that the transition probability from state  $S$  to state  $S'$  with the  $C'_{\max} = C_{\max}$  is simply  $P_{\text{cas}}(S, R_{D/G}) \times P_{E_W}$ . However, the event  $E_U$  can lead the initial state to transit to different possible states. Conditioning on the occurrence of the event  $E_U$ , the possible events  $E_{U_i|U}$  where  $i \in \mathcal{I}$  may occur. With the probability of these events,  $P_{E_{U_i|U}}$ , the transition probability from state  $S$  to a state  $S'$  (with  $C'_{\max} > C_{\max}$ ) is  $P_{\text{cas}}(S, R_{D/G}) \times P_{E_U} \times P_{E_{U_i|U}}$ .

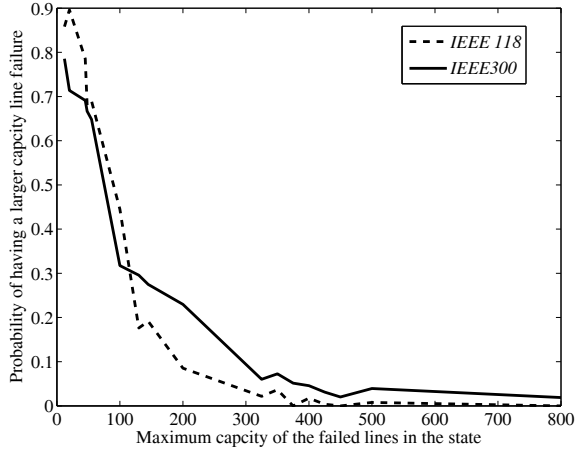


Fig. 5. Probability of event  $E_U$  as a function of maximum capacity of the failed lines in the initial state.

Using the simulated data sets and the procedures outline above, we have calculated the probability of occurrence of event  $E_U$ . In Fig. 5, we show the probability of the events  $E_U$  as a function of maximum capacity of the failed lines in the states. The probability of the event,  $E_W$ , is one minus the probability of event  $E_U$ , i.e.,  $P_{E_W} = 1 - P_{E_U}$ .

Now assuming that the event  $E_U$  has occurred, we present in Fig. 6 the transition probability from state  $S$  to different possible states  $S'$  with  $C'_{\max} > C_{\max}$ . Based on the result presented in Fig. 6, we can deduce that the probability of transiting from a state  $S$  to states  $S'$  with  $C'_{\max} > C_{\max}$  decreases as the difference of the  $C'_{\max}$  and  $C_{\max}$  increases. This is meaningful since when a line outage occurs, it is more likely that it affects other lines with capacity values close to its own capacity, rather than a line with much larger capacity than its own. We model this behavior by the right half side of a Gaussian function centered at the  $C_{\max}$  value for state  $S = (C_{\max}, F)$ . The properties of the formed Gaussian functions are different for the states with different  $C_{\max}$  values. In order to approximate the pdfs in Fig. 6, we set larger variances and lower heights for the Gaussian functions of the states with smaller  $C_{\max}$  values than the states with larger  $C_{\max}$  values. In other words, as  $C_{\max}$  increases the Gaussian variance reduces and its height increases. The transition rates are calculated

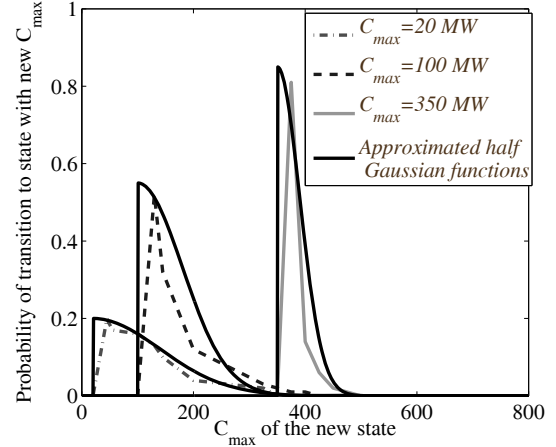


Fig. 6. The transition probability from three initial states with different maximum capacity of the failed lines to different possible states  $S'$  with  $C'_{\max} > C_{\max}$ .

from the transition probabilities. We omit the details of these calculations.

## V. RESULTS

In this section, we solve the set of coupled differential equations presented in (4) with the initial conditions presented in (5) for the IEEE 118-bus system.

The probabilities of blackouts with size  $M = 40$  (21.5% of the total grid size) or larger, as a function of time, are presented for representative initial grid states and  $R_{D/G}$  values in Fig. 7. As can be seen in Fig. 7 and also stated in past blackout reports [3], the cascading failures phenomena have two phases in time. In the beginning, the cascade of events are slow. After passing this initial phase, if no action is taken to protect the power grid and prevent more failures, the cascading failure phenomena reach a new phase in time where the cascade of failures occur rapidly.

The results presented here are for scenarios with multiple initial failures and for different maximum capacity of the failed lines. In Fig. 7-a and Fig. 7-b we assume that the grid operates at half of its maximum capacity,  $R_{D/G} = 50\%$ . In the other two plots in Fig. 7, we assume that  $R_{D/G} = 90\%$  which means that the grid is operating close to its maximum capacity. The results presented in Fig. 7-a and Fig. 7-c are for an initial grid state with five failures, and the results in Fig. 7-b and Fig. 7-d are for initial grid states with ten failures. Notice that in cases where the maximum capacity of the failed lines is large ( $> 400MW$ ), the probabilities of the blackouts are larger than those corresponding to other cases where the maximum capacity is low. The same effect can be seen when the number of initial failures is large. As expected, in cases where the grid-loading ratio is large the probabilities of blackouts are also large compared to those with smaller values of the grid-loading ratio. Moreover, the probability increases much faster in time than other initial grid states. These plots represent evolution of the risk of blackout in time and how quickly the risk increases with time if no action is taken as time passes. The results are consistent with the physical concepts used in

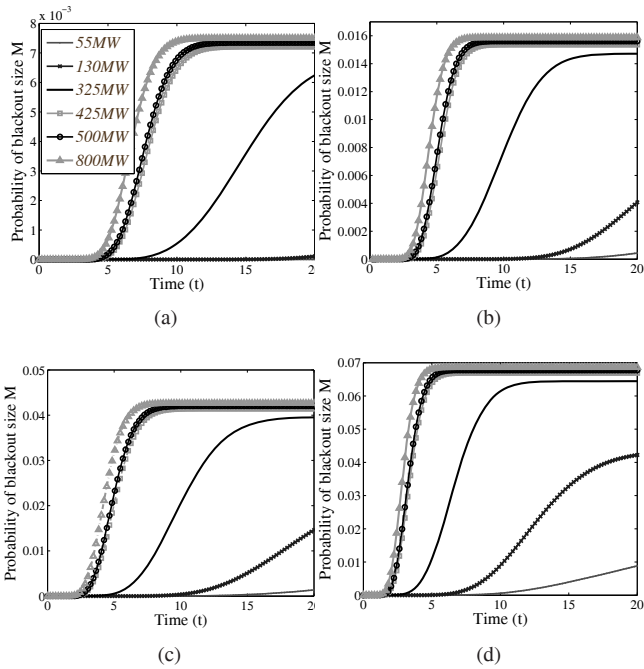


Fig. 7. Calculated values of the probability of reaching blackouts with size  $M = 40$  or more in the IEEE 118-bus system in the 20 minutes time interval. Each curve in each subplot is parameterized by the maximum capacity of the failed lines. (a) Initial state has 5 failures and  $R_{D/G} = 50\%$ , (b) initial state has 10 failures and  $R_{D/G} = 50\%$ , (c) initial state has 5 failures and  $R_{D/G} = 90\%$ , and (d) initial state has 10 initial failures and  $R_{D/G} = 90\%$ .

the model and also simulation results presented in Section III and Section IV-C.

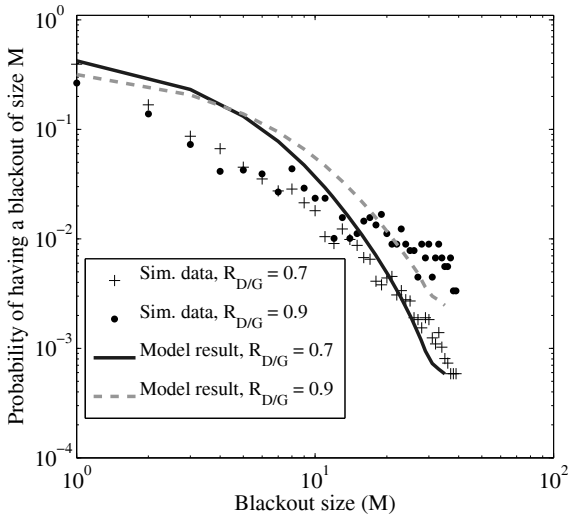


Fig. 8. Probability of having a blackout of size  $M$ , as a function of  $M$ , for the IEEE 118-bus system. Solid and dashed lines represents the results calculated from our model and the dots and crosses represent estimates obtained using Monte Carlo simulations over the IEEE 118-bus system.

We have also derived the probability of a blackout of size  $M$  within a time window of 30 minutes, as a function of  $M$ . To calculate these probabilities at each value of  $M$ , we extract the calculated probabilities from the model with the specific time interval,  $t = 30$ . In particular, the value of the

probability of a blackout of size  $M$  within a time window of 30 minutes is  $B_{(C_{\max}, F)}^{R_{D/G}}(30, M) - B_{(C_{\max}, F)}^{R_{D/G}}(30, M + 1)$ , which yields the probability mass function of the blackout size. The results calculated from our model are shown in Fig. 8 (solid and dashed lines) and they are in agreement with the results obtained from the Monte Carlo simulations over the IEEE 118-bus system. The presented results are for two grid-loading ratio values,  $R_{D/G} = 70\%$  and  $R_{D/G} = 90\%$ .

## VI. CONCLUSIONS

Understanding cascading failures and the ability to predict the risk of blackouts are of great value in designing control and outage management systems in future smart grids. In this paper, we presented a probabilistic regeneration-based model for the dynamics of cascading failures. This model is a step toward using the physical factors of the power system in improving the understanding of cascading failures. The proposed model characterizes the probability of reaching a blackout of an arbitrary size in any time interval starting from an initial grid state. The parameters of the model are estimated by means of Monte Carlo simulations.

We attempted to address the challenges in modeling cascading failures, namely the complexity of cascading failure phenomena and the scalability of the model to large grids. To do so, we identified and exploited a limited number of physical factors from the power grid, which have critical roles in cascading failures. To this end, we used the number of transmission line failures as well as the maximum capacity of the failed lines to dramatically reduce the space of all possible grid configurations into a smaller set of equivalence classes. Our approach is therefore scalable to large realistic power grids that may have in excess of thousands of lines. Our preliminary results suggest that the cascading failures models can be further enhanced by considering more key factors contributing to cascading failures. This approach enhances the prediction of the risk of blackouts, which enable cascading-failure-aware control and management policies for future smart grids. Considering the effects of corrective and remedial control actions in the cascading failures model can be an extension of the presented work.

## VII. APPENDIX

**Derivation of Renewal Equations:** Consider the equation in (4). By exploiting the fact that the minimum of independent exponential random variables is also an exponential random variable, we obtain  $f_\tau(t) = \lambda(S, R_{D/G})e^{\lambda(S, R_{D/G})t}$ , where  $\lambda(S, R_{D/G}) = \lambda_W(S, R_{D/G}) + \sum_i \lambda_{U_i}(S, R_{D/G})$ . Further,  $P\{\tau = W | \tau = s\} = \frac{\lambda_W(S, R_{D/G})}{\lambda(S, R_{D/G})}$ , and  $P\{\tau = U_i | \tau = s\} = \frac{\lambda_{U_i}(S, R_{D/G})}{\lambda(S, R_{D/G})}$ . Now, if we substitute the conditional probabilities presented in (3) together with the above probabilities in the equality presented in (4), we determine the integro-difference

equation,

$$\begin{aligned}
B_{(C_{\max}, F)}^{R_{D/G}}(t, M) &= \left(1 - P_{\text{stab}}(S, R_{D/G})\right) \\
&\times \int_0^t \left(\lambda_W(S, R_{D/G}) B_{(C_{\max}, F+1)}^{R_{D/G}}(t-s, M)\right. \\
&\left. + \sum_{i \in \mathcal{I}} \lambda_{U_i}(S, R_{D/G}) B_{(C_{\max}, F+1)}^{R_{D/G}}(t-s, M)\right) e^{-\lambda(S, R_{D/G})s} ds.
\end{aligned} \tag{6}$$

By using the Leibnitz integral rule and change of variables, it is easy to show that the derivative of (6) is (4).

#### ACKNOWLEDGMENT

This work was supported by the Defense Threat Reduction Agency (contract no. DTRA01-03-D-0009-0026, University Partnership Program: Fundamental Research). The authors wish to thank Shahin Abdollahy, Yasser Yasaei, and Yasamin Mostofi for valuable discussions.

#### REFERENCES

- [1] N. D. Dobson I, Carreras BA, "A loading-dependent model of probabilistic cascading failure," *Probability in the Engineering and Informational Sciences*, vol. 19, no. 1, 2005.
- [2] M. Anghel, K. A. Werley, and A. E. Motter, "Stochastic model for power grid dynamics," in *40th Annual Hawaii International Conference on System Sciences, HICSS*, Jan. 2007.
- [3] G. Andersson, P. Donalek, R. Farmer, N. Hatziaargyriou, I. Kamwa, P. Kundur, N. Martins, J. Paserba, P. Pourbeik, J. Sanchez-Gasca, R. Schulz, A. Stankovic, C. Taylor, and V. Vittal, "Causes of the 2003 major grid blackouts in north america and europe, and recommended means to improve system dynamic performance," *IEEE Transactions on Power Systems*, vol. 20, no. 4, pp. 1922 – 1928, Nov. 2005.
- [4] R. Adler, J. Daniel, S.L., C. Heising, M. Lauby, R. Ludorf, and T. White, "An ieeec survey of us and canadian overhead transmission outages at 230 kv and above," *IEEE Transactions on Power Delivery*, vol. 9, no. 1, pp. 21 –39, Jan. 1994.
- [5] D. Newman, B. Carreras, V. Lynch, and I. Dobson, "Exploring complex systems aspects of blackout risk and mitigation," *IEEE Transactions on Reliability*, vol. 60, no. 1, pp. 134 –143, Mar. 2011.
- [6] B. A. Carreras, V. E. Lynch, I. Dobson, and D. E. Newman, "Critical points and transitions in an electric power transmission model for cascading failure blackouts," *Chaos*, vol. 12, 2002.
- [7] I. Dobson, B. Carreras, and D. Newman, "Branching process models for the exponentially increasing portions of cascading failure blackouts," in *38th Annual Hawaii International Conference on System Sciences, HICSS*, Jan. 2005.
- [8] I. Dobson, K. Wierzbicki, J. Kim, and H. Ren, "Towards quantifying cascading blackout risk," in *Bulk Power System Dynamics and Control - VII. Revitalizing Operational Reliability, iREP Symposium*, Aug. 2007.
- [9] J. Kim and I. Dobson, "Approximating a loading-dependent cascading failure model with a branching process," *IEEE Transactions on Reliability*, vol. 59, no. 4, pp. 691 –699, Dec. 2010.
- [10] D. Daley and D. Vere-Jones, *An Introduction to the Theory of Point Processes*, 2nd ed. Springer, 2003.
- [11] F. Baccelli and P. Bremaud, *Queueing Theory: Palm-Martingale Calculus and Stochastic Recurrence*. Springer-Verlag, 1994.
- [12] Q. Chen and J. D. McCalley, "A cluster distribution as a model for estimating high-order-event probabilities in power systems," *Probab. Eng. Inf. Sci.*, vol. 19, pp. 489–505, Oct. 2005.
- [13] H. Ren, I. Dobson, and B. Carreras, "Long-term effect of the n-1 criterion on cascading line outages in an evolving power transmission grid," *IEEE Transactions on Power Systems*, vol. 23, no. 3, pp. 1217 –1225, Aug. 2008.
- [14] V. L. P. Crucitti and M. Marchiori, "Model for cascading failures in complex networks," *Physical Review E*, vol. 69, no. 4, 2004.
- [15] C. L. DeMarco, "A phase transition model for cascading network failure," *IEEE Control Systems Magazine*, vol. 21, no. 6, pp. 40–51, Dec. 2001.
- [16] R. Baldick *et al.*, "Initial review of methods for cascading failure analysis in electric power transmission systems ieeec pes cams task force on understanding, prediction, mitigation and restoration of cascading failures," in *Power and Energy Society General Meeting - Conversion and Delivery of Electrical Energy in the 21st Century*, July 2008.
- [17] R. Zimmerman, C. Murillo-Sanchez, and D. Gan, *MATLAB Power System Simulation Package*, version 4.0b4 ed., May 2010.
- [18] J. D. Glover, M. S. Sarma, and T. J. Overbye, *Power system analysis and design*, 4th ed. Cengage Learning, 2008.